JIEE Časopis priemyselnej elektrotechniky
Journal of Industrial Electrical Engineering
ISSN 2454-0900
www.jiee.eu

Design of a current source for the magnetization of single-sheet magnetoelastic sensors

[1]*Šimon GANS*, [2]*Ján MOLNÁR*

[1,2] Department of Theoretical and Industrial Electrical Engineering, Faculty of Electrical Engineering and Informatics, Technical university of Košice, Slovakia

[1]simon.gans@tuke.sk, [2]jan.molnar@tuke.sk

***Abstract* — This work addresses the problem of designing a current source that supplies electric current to the primary (or magnetizing) winding of a magnetoelastic sensor. Firstly, a simulation model was set up in the Proteus 8 Professional simulation program where multiple variations of the current source were tested. The best-performing one is described in this paper. The current source was constructed on a breadboard and after final adjustments, it was soldered to a prototyping board.**

***Keywords* — bipolar transistor, current, operational amplifier, magnetization.**

I. INTRODUCTION

Magnetoelastic sensors are based on the effect of changing magnetic material properties due to the action of internal or external stresses [1]. A magnetization of the material ***M*** must exist either due to permanent magnets for biasing [2] or magnetizing coils [3]. Usually, only magnetizing coils are used [4]. Using coils allows for time-varying magnetization waveforms depending on the current waveform. This allows for the continuous measurement of even static forces [1]. When using permanent magnets the flux change through the sensing coil would need to be integrated over time continuously which would yield large errors over time and is used only for dynamic measurements [5].

During magnetization, a predefined waveform must be used in every cycle. Due to the hysteretic behavior of magnetic materials changing the derivative of the current during the magnetization period can change the path traced on the hysteresis loop which in turn changes the induced voltage waveform slightly due to the current variation [6]. Such variations can be unpredictable if the current regulation is not precise enough, and therefore variations in every period are present.

Electrical steels used for the construction of such sensors have a high value of electrical conductivity which makes eddy currents a significant factor during the magnetization process at higher frequencies [7]. From experimental testing, it was found that a current frequency limit of 1 kHz is the upper bound before eddy currents start to significantly affect the magnetization process [8].

II. SCHEMATIC OF THE CURRENT SOURCE

For the current source the following schematic was used shown in Fig. 1. A non-inverting operational amplifier [9] U4:A is used to amplify the voltage drop signal created by the flow of current through the shunt resistor R_{11}. The amplified signal is then compared with a voltage signal created by a voltage generator that defines the current waveform. The output of the comparator U1:B is equal to V+, when the current flowing through the magnetizing coil is lower than its desired value and equal to V- if it is higher. This voltage signal (that creates a current flow) is supplied to the bases of two complementary bipolar transistors placed on heat sinks that regulate the flowing current.

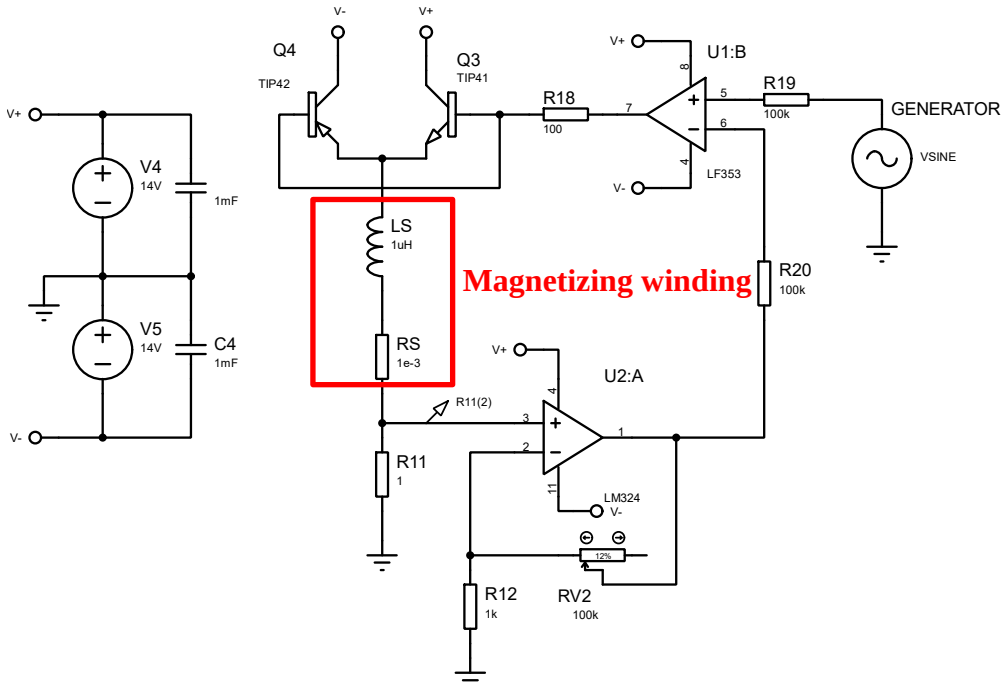

Fig. 1: Schematic of the current source

In the pictures below (Fig. 2 and Fig. 3) simulations are shown for sine and triangular waveforms.

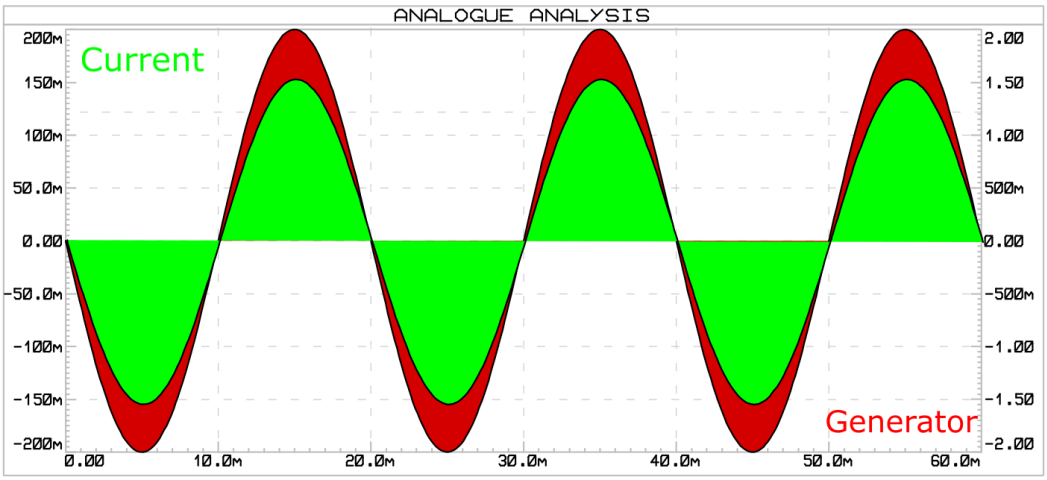

Fig. 2: The sinusoidal current waveform with a frequency of 50 Hz and an amplitude of 150 mA created by a sinusoidal voltage signal with an amplitude of 2 V.

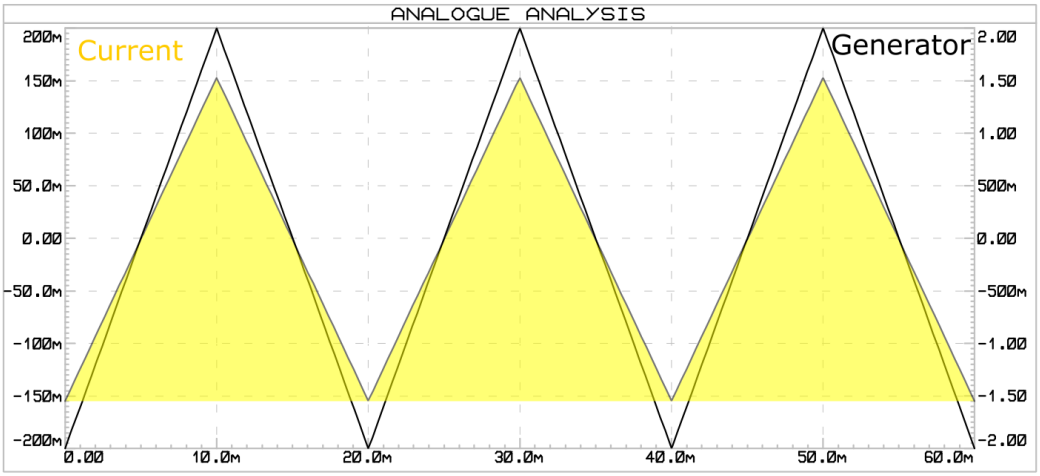

Fig. 3: The triangular current waveform with a frequency of 50 Hz and an amplitude of 150 mA created by a triangular voltage signal with an amplitude of 2 V.

All operational amplifiers are powered by a symmetrical ±12V power supply with two 1 mF smoothing capacitors. Every operational amplifier has a filtering capacitor present near its power supply pins consisting of a combination of an electrolytic and a ceramic capacitor. The magnetizing winding is represented in the schematic by a resistor and an inductor connected in series. It must be said that the inductance of the magnetizing winding will change during magnetization due to the magnetic material nonlinearity, which manifests itself as different permeabilities at different magnetizing currents [6].

When a square wave signal with an amplitude of 2V is used as the generator signal with varying rising and fall times the following current graphs were obtained (Fig. 4 to Fig. 6). It is evident that oscillations can occur after the transition level depending on the speed of the change. This is mainly caused by the inductance of the primary winding. The sine and triangle current waveforms however do not seem to be hard to regulate accurately at the frequency of 50 Hz.

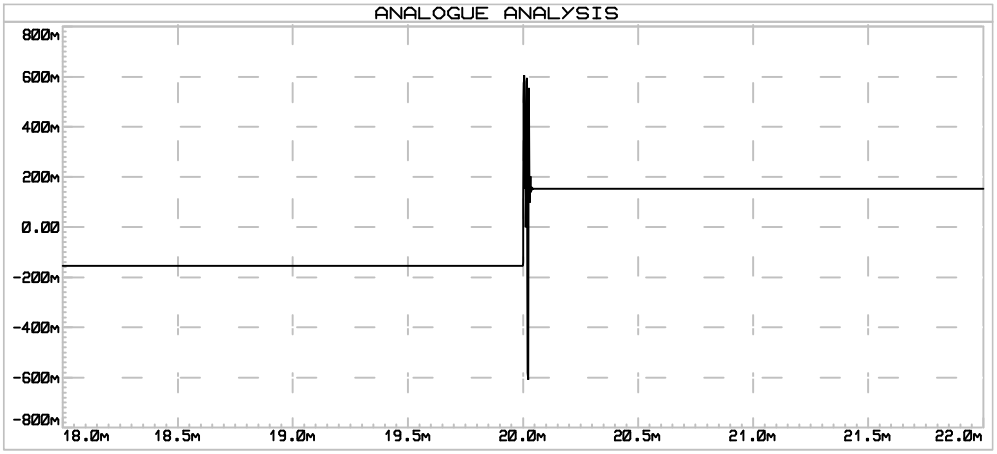

Fig. 4: The rising edge of the current waveform created by a square wave generator signal with 10µs rise and fall time.

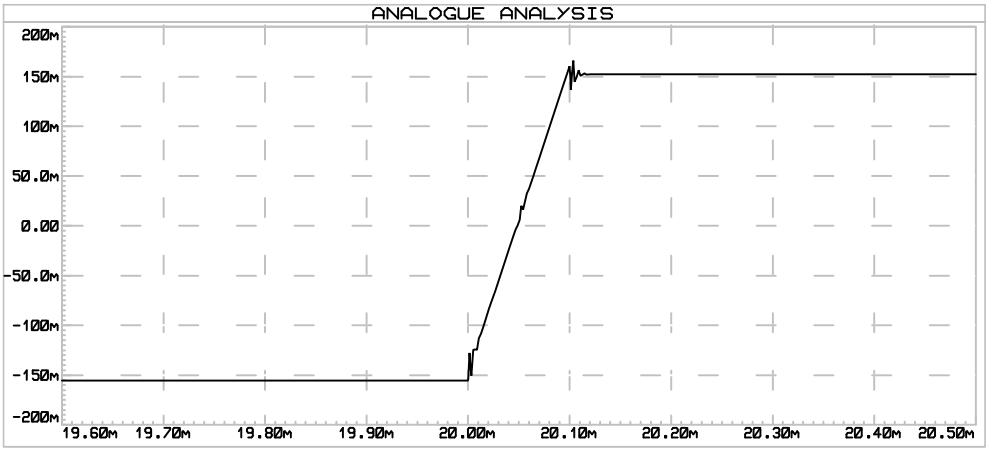

Fig. 5: The rising edge of the current waveform created by a square wave generator signal with 100µs rise and fall time.

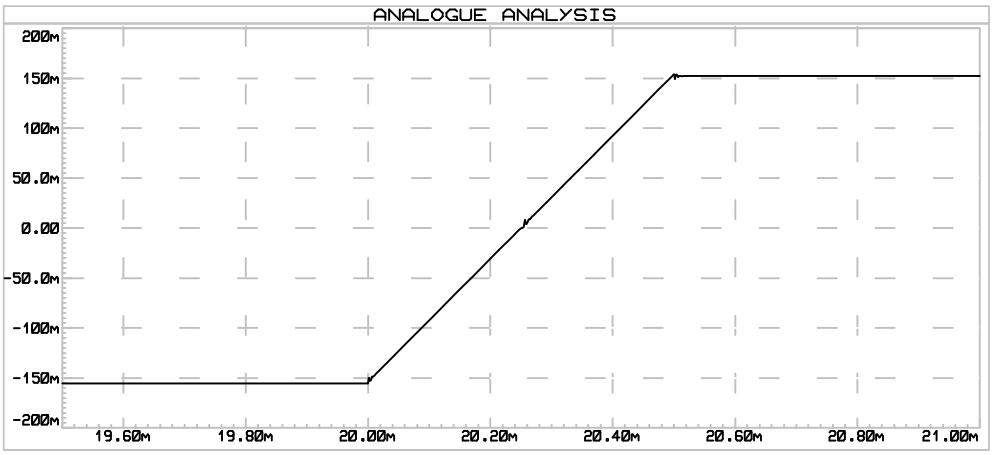

Fig. 6: The rising edge of the current waveform created by a square wave generator signal with 500µs rise and fall time.

III. PROTOTYPE MANUFACTURE

The transistors used were TIP41C and TIP42C which have a maximum collector current of 6A, which therefore limits the current source output ability to these values. However, the bases of the transistors are controlled by the output of the operational amplifier, which depending on the type and the output impedance limits the base current. The transistors have a relatively low h_{21E} value of approximately 30 to 75. The LF353 operational amplifier has a short circuit current of approx. 60 mA, which means that it can drive the transistors to regulate currents from 1,8 A to 4,5 A, which should be sufficient for most applications. The full range of the source will be tested. All operational amplifiers are powered by a symmetrical ±12V power supply with two 1 mF smoothing capacitors.

The connections were made on a breadboard and component values were tested for the best performance regarding the stability of the generated waveform. After finding suitable component values the setup was soldered to a prototyping board which made the connections more rigid (Fig. 7).

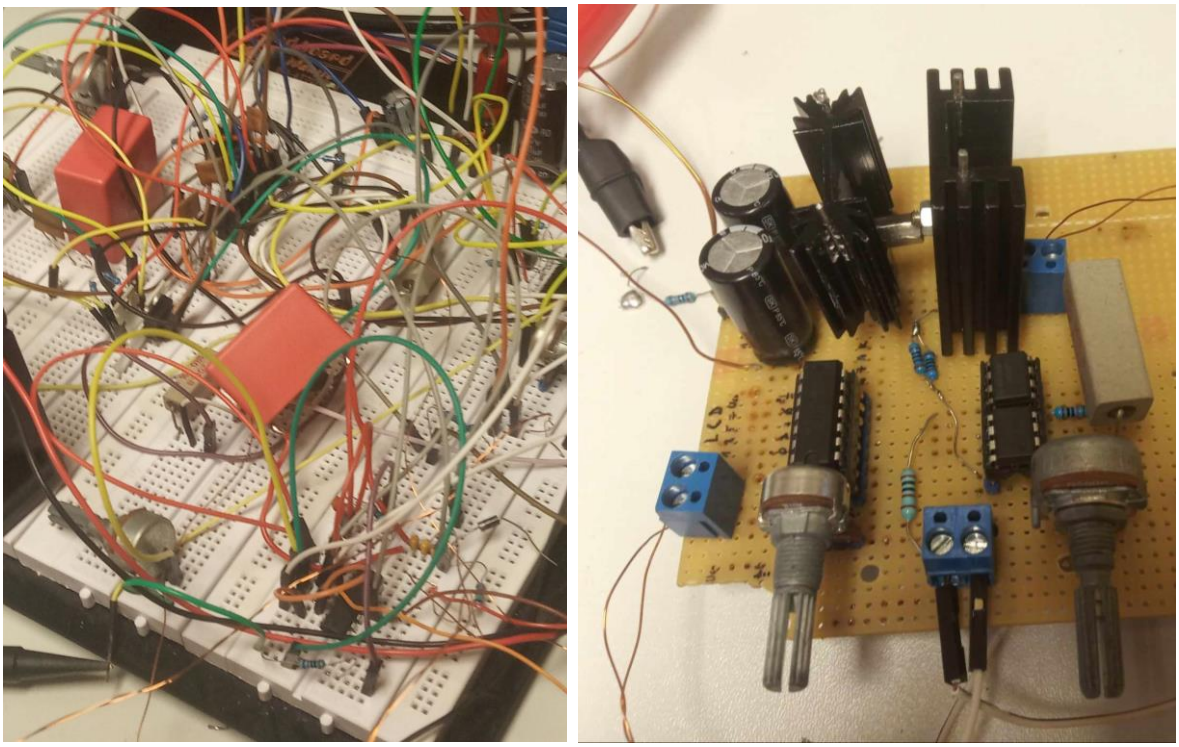

Fig. 7: The prototype of the current source on a breadboard (left) and soldered to a prototyping board (right).

The filtering capacitors and the wires for the connection have been placed from the underside of the board which is shown in (Fig. 8). An external fan was added to cool the transistors' heatsinks during operation. The used capacitors for the operation amplifier voltage filtering were a combination of 220 µF electrolytic capacitors and 100 nF ceramic capacitors. For the input voltage filtering two 1000 µF electrolytic capacitors were used.

The magnetoelastic sensor consisted of two perpendicular coils, one magnetizing and one sensing (Fig. 9). The magnetizing winding consists of 12 turns of enameled copper wire with a circular cross-section with a diameter of 0,3 mm. The inductance and equivalent series resistance (ESR) of the coil were measured on an LCR meter at a testing frequency of 50 Hz. The inductance of the coil was 53,675 µH and its resistance was 243,02 mΩ.

In the final version of the current source the operational amplifier for the voltage sensing amplification an OP07CP amplifier was used because of its lower input offset temperature dependence compared to the LM324. During operation with the LM324 amplifier when the cooling fan was turned on a visible voltage change of its output voltage at a constant input voltage was observed. This was mitigated by the change of the operational amplifier.

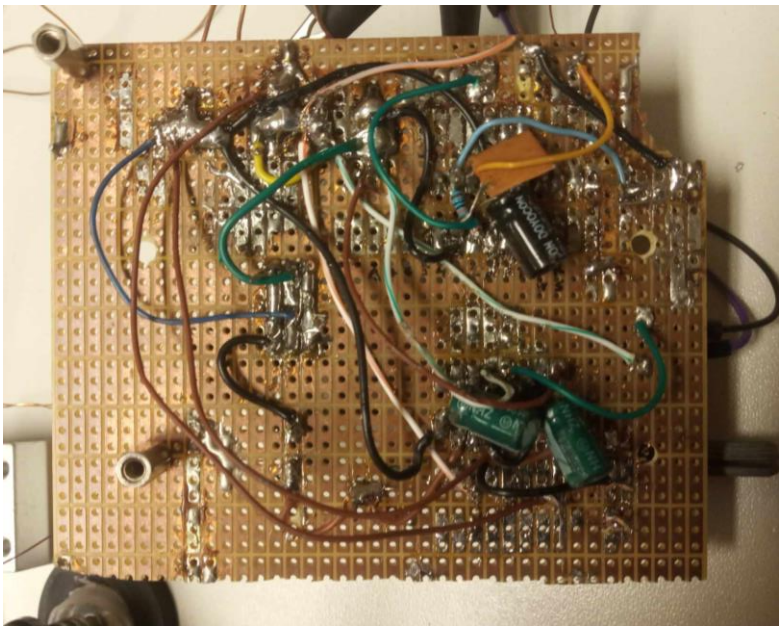

Fig. 8: Under side of the prototyping board with the filtering capacitors.

Fig. 9: The magnetoelastic sensor with the highlighted magnetizing winding.

The relationship between the control voltage and the output current is given by eq. (1). The gain of the current source is adjustable by controlling the current sensing amplifier gain by the potentiometer RV_2.

$$i(t) = u(t) \cdot \left(1 + \frac{RV_2}{R_{12}}\right) \cdot R_{11} \tag{1}$$

IV. TESTING OF THE CURRENT SOURCE

During the testing of the current source sinusoidal, triangular and square wave control signals with an amplitude of 500 mV were used at frequencies of 50 Hz, 500 Hz, 1 kHz and 5 kHz. The current source was set to generate output current with an amplitude of 200 mA. The current signal through the magnetizing winding was measured with a hall probe connected to a Tektronix oscilloscope with the channel set to a 300 mA measurement range. The following graphs were measured (Fig. 10 to Fig. 13). A slight nonlinearity can be observed at frequencies of 1 kHz and 5kHz near the zero-crossing that arose during the operation transition from one bipolar transistor to the other. However as it was analyzed in the introduction the upper frequency limit of the current source for the given application is 1 kHz which means that the current source sufficiently performs the desired task.

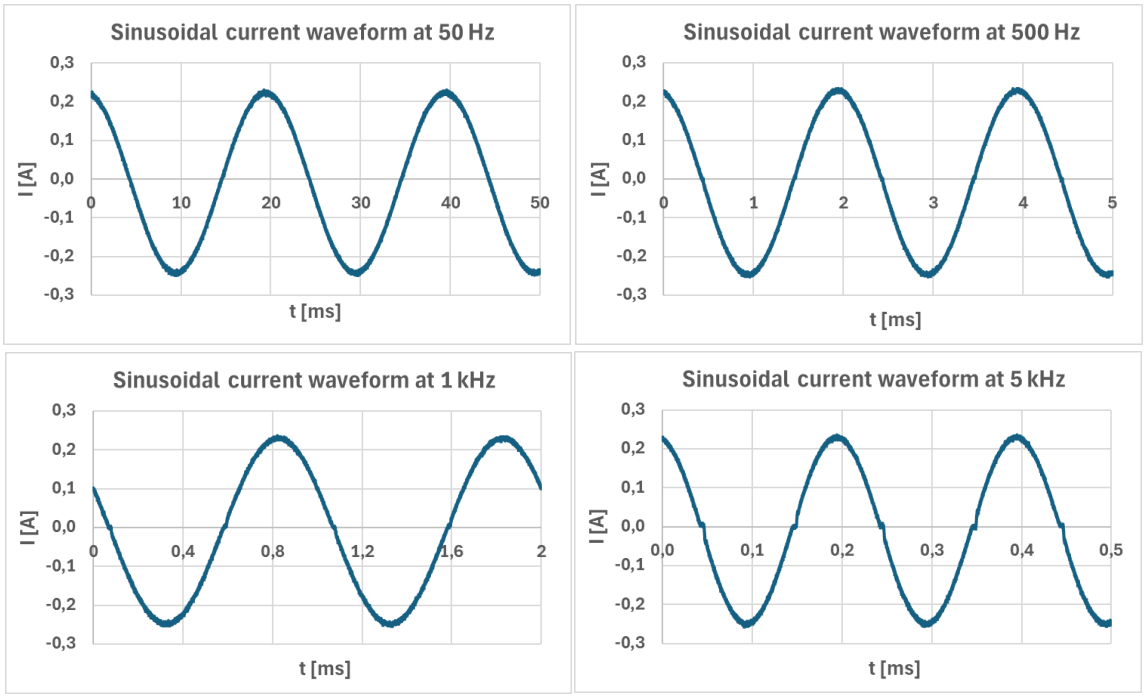

Fig. 10: Generated sinusoidal current waveforms at various frequencies.

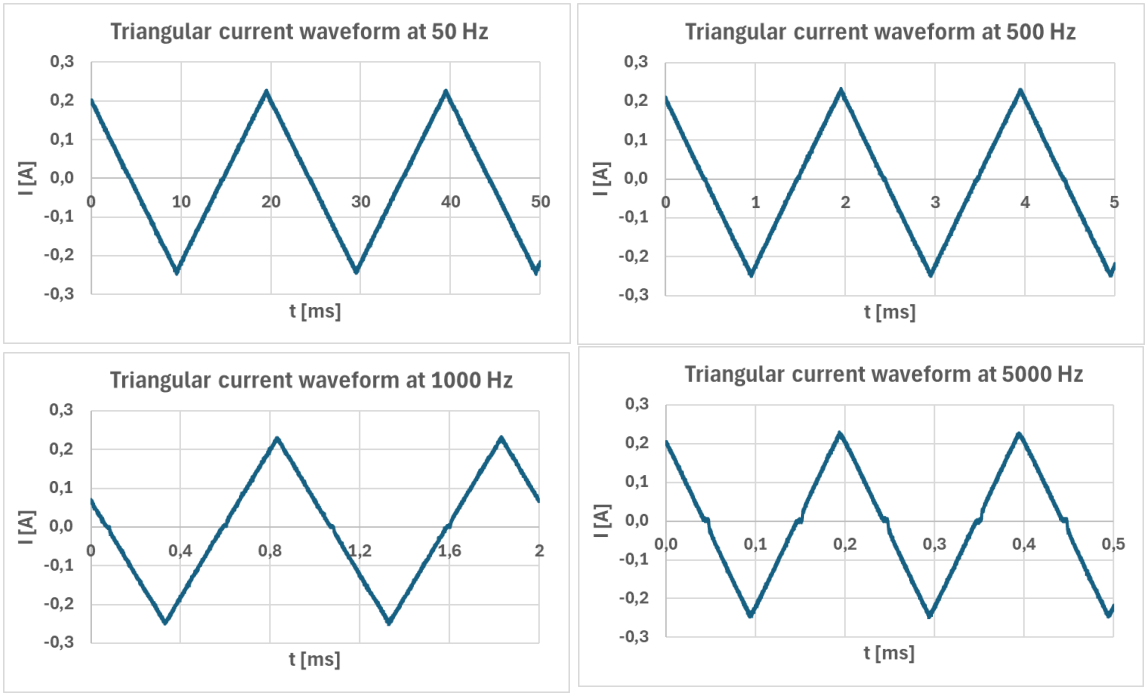

Fig. 11: Generated triangular current waveforms at various frequencies.

The 50 Hz square waveform had a slight peak right after the transition zone which is less pronounced at higher frequencies probably because it lasts the same time, but the length of the period changes.

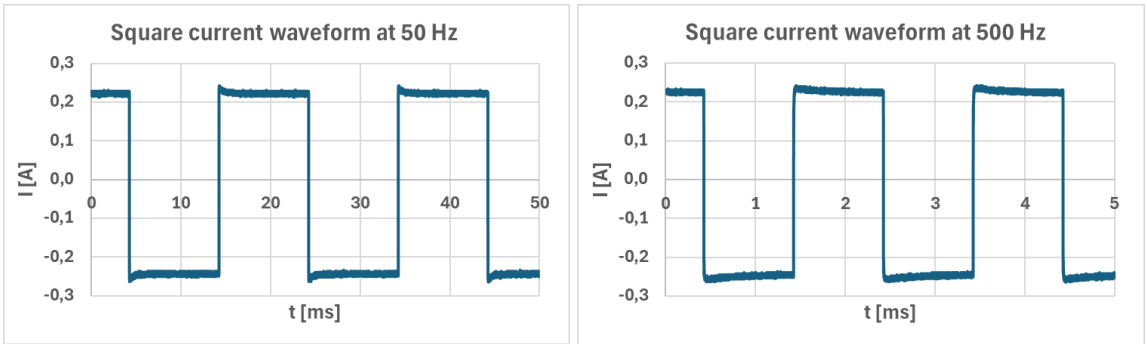

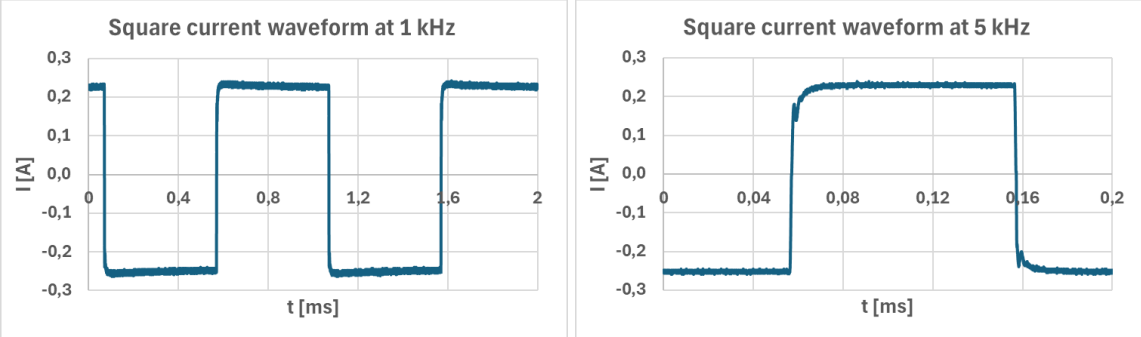

Fig. 12: Generated square current waveforms at various frequencies.

Even in the 50 Hz square wave current signal during the transitions zone a 5 µs transient is present. This can be further mitigated by decreasing the falling and rise times of the square wave control signal, but for this usage the current regulating accuracy of the source is sufficient for frequencies under 1 kHz.

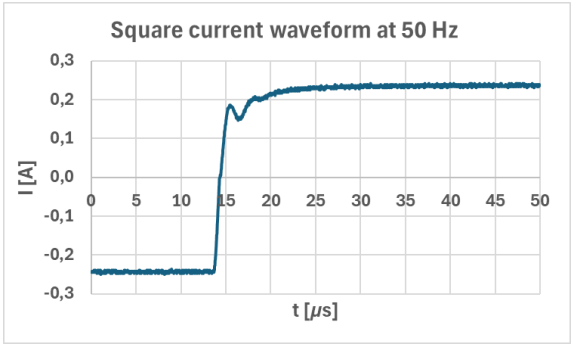

Fig. 13: Detail of the square wave current at the transition zone. A 5µs oscillation can be observed.

The current source was powered by a symmetrical ±12 V power supply during testing. The largest tested output current amplitude was 2 A. The source could handle larger currents due to the power transistors, but an upgrade of the heatsinks should be done. After testing the source with a 3 A current amplitude one transistor in the design overheated and was destroyed.

V. Conclusion

A current source was created for the magnetization of magnetoelastic sensor samples. The requirements placed on its design were to supply various periodic current waveforms with a frequency of up to 1 kHz and an amplitude of at least 1 A. The performance of the current source was deemed to be sufficient. No deformation of the generated sinusoidal and triangular waveforms were observed in the given frequency band. The square waveforms had some ringing present during the transition zones from one current level to another depending on the rise and fall times.

The device is simple and does not need many adjustments since the magnetizing winding has only a relatively low value of inductance. For a better operation one could place a low value resistor in series with the magnetizing winding which would make the entire load act more like an resistor and less like an inductor. Regulating the current flowing through resistive loads is simpler than doing so inductive loads since there is no phase shift (or delay) between the current and voltage applied to it.

For the optimal operating efficiency of the current source the supply voltage should be as low as possible. The transistors regulate the flow of current by dropping enough voltage between their collector and emitter from the supply voltage so that the given voltage on the load creates the desired current flow. The higher voltage is dropped on the transistors the higher the power losses will be. But the supply voltage must be high enough to ensure the correct operation of the operational amplifiers since it defines their output voltage ranges.

References

[1] Dahle O., The Pressductor and the Torductor – Two Heavy-Duty Transducers Based on Magnetic Stress Sensitivity, IEEE Transactions on Communication and Electronics, 1964, vol. 83, issue 75, doi: 10.1109/TCOME.1964.6592601. Available on the internet at: https://ieeexplore.ieee.org/abstract/document/6592601

[2] Deng Z., Dapino M. J., Magnetic flux biasing of magnetostrictive sensors, IOP Publishing, Smart materials and Structures, 2017, 26, 055027, doi: 10.1088/1361-665X/aa688b. Available on the internet at: https://iopscience.iop.org/article/10.1088/1361-665X/aa688b

[3] Bieńkowski A., Szewczyk R., Salach J., Industrial Application of Magnetoelastic Force and Torque Sensors, 14th Czech and Slovak Conference on Magnetism, Košice, Slovakia, July 6-9, 2010, Acta Physica Polonica A, vol. 118, no. 5, doi: 10.12693/APhysPolA.118.1008. Available on the internet at: http://przyrbwn.icm.edu.pl/APP/PDF/118/a118z5p120.pdf

[4] Bydzovsky J., Kollár M., Kraus L., Svec P., Linearization of two-coil magnetoelastic sensor transfer characteristic, Journal of Electrical Engineering, 2004, 55(10):62-65. Available on the internet at: https://www.researchgate.net/publication/228418902_Linearization_of_two-coil_magnetoelastic_sensor_transfer_characteristic

[5] Skinner W. S., Zhang S., Guldberg R. E., Ong K. G., Magnetoelastic Sensor Optimization for Improving Mass Monitoring, MDPI Sensors, 2022, 22(3), 827, doi: 10.3390/s22030827. Available on the internet at: https://www.mdpi.com/1424-8220/22/3/827

[6] Hajko V., Potocký L., Zentko A., Magnetizačné procesy, Vydavateľstvo technickej a ekonomimckej literatúry Alfa Bratislava, 1. Vydanie, 63-119-82

[7] Elgamli E., Anayi F., Advancements in Electrical Steels: A Comprehensive Review of Microstructure, Loss Analysis, Magnetic Properties, Alloying Elements, and the Influence of Coatings, MDPI Applied Sciences, 2023, 13(18), doi: 10.3390/app131810283. Dostupné na internete na: https://www.mdpi.com/2076-3417/13/18/10283?type=check_update&version=2

[8] Gans Š., Molnár J., Kováč D., Kováčová I., Fecko B., Bereš M., Jacko P., Dziak J., Vince T., Driving Signal and Geometry Analysis of a Magnetoelastic Bending Mode Pressductor Type Sensor, MDPI Sensors, 2023, 23(20), doi: 10.3390/s23208393. Dostupné na internete: https://www.mdpi.com/1424-8220/23/20/8393

[9] Electronics tutorials, Non-inverting operational amplifier. Available on the internet at: https://www.electronics-tutorials.ws/opamp/opamp_3.html